MULTI-DISCIPLINARY DESIGN EXPLORATION FOR WINGLET

Keizo Takenaka*, Keita Hatanaka*, Kazuhiro Nakahashi**
*MITSUBISHI AIRCRAFT CORPORATION, 2-15, Oye-cho, Minato-Ku, Nagoya, 455-8555 Japan
**Tohoku University 6-6-1, Aoba, Aoba-ku, Sendai, 980-8579, Japan

Keywords:*MDO, Winglet, ANOVA, Kriging*

Abstract

In this paper, we describe a multi-disciplinary design exploration technique applied to the winglet design for a commercial jet aircraft. Minimization of block fuel at a fixed aircraft operating range and maximum takeoff weight were selected as design objectives. Both objective functions were estimated from CFD based aerodynamic drag and FEM based structural weight. Various CFD and optimization techniques such as mid-field drag decomposition method, automatic CFD mesh generation, Kriging surrogate model and Multi-Objective Genetic Algorithms were integrated and applied for the detail design exploration. CFD with the mid-field drag decomposition method showed the effect on drag components of wave, induced and profile drag due to different winglet defining parameters. Practical design decision was explored based on the Pareto front and some design criteria that were uncovered within the numerical optimization. Finally, the design process was validated through the validation of the Kriging approximation and aerodynamic characteristics based on the wind tunnel test.

1 Introduction

Winglet has been widely used on commercial aircraft as a means of enhancing fuel efficiency. Winglet, originally designed as add-on devices for existing airplanes, has now become an essential part of aircraft design. The initial concept of the winglet was demonstrated experimentally (Ref.[1]). Wind tunnel, flight tests and the database constructed by previous tests have been the main tools for the designers. Then, computational methods, such as the panel method were utilized for more efficient design of the winglet in the early design phase (Ref.[2]). Most of previous designers focused on induced drag reduction (Ref.[3]) in the early design phase. Effects on the other drag components of profile and wave drag were mainly confirmed by wind tunnel test as the next design step. Also structural design considerations, such as weight penalty and flutter characteristics were considered in the structural design phase in a sequential manner.

Recently, thanks to the advancement of Computational Fluid Dynamics (CFD), Computational Structural Dynamics (CSD) and Multi-disciplinary Design Optimization (MDO) techniques, innovative design tools for the designer are available.

The reduction in airplane drag by the winglet is on the order of 10 drag counts (1drag count = 1×10-4), and incremental drag due to the winglet shape trade-off is on the order of 1 drag counts (about 0.3% of the airplane total drag at cruise). These orders of drag estimation by CFD are tend to be unreliable because of the effect of computational mesh dependency. Therefore, accurate drag prediction is essential for the reliable winglet shape design. Another difficulty in winglet design is that it includes the variation of each drag component, such as wave, profile and induced drag. The installation of the winglet will cause induced drag reduction because of the increase in the wing span, wave drag generation around the wing-winglet junction, and additional profile drag because of the increase in the wetted area. Therefore, the behavior of each drag component has to be discussed in detail for the advanced winglet design. Recently, as an advanced drag prediction method, the mid-field drag decomposition method (Ref. [4]-[7]) has attracted much attention. In the mid-field

method, the spurious drag component, which is generated by the spurious entropy production due to numerical diffusion, can be computed and eliminated from the total drag. This enables more accurate drag prediction. By using the mid-field method, the total drag can be decomposed into three physical components of wave, profile and induced drag, and one spurious drag component. This advanced analysis approach will achieve more reliable aerodynamic shape optimization of winglet.

In this paper, we discuss the multi-disciplinary design exploration technique with high-fidelity CFD as applied to the winglet design of a commercial jet aircraft for the advanced winglet design. Effectiveness and efficiency of the high-fidelity MDO technologies to the practical aircraft design is discussed.

2 Design process and applied technologies

2.1 Design problem definition and overview of the design process

In the present study, we conducted winglet design for wing-body configuration of a commercial jet. Minimization of the block fuel derived from aerodynamic drag and structural weight was selected as an objective function. The block fuel is defined as the minimum fuel mass for a fixed range. In addition, minimization of Max Take Off Weight (MTOW), which is related to the airport landing fee charged in some airports for commercial jets, was considered as another objective function.

There are many optimizers such as genetic algorithms (Ref.[8]), adjoint method (Ref.[9]) and Kriging surrogate model based optimization (Ref.[10]). The Kriging model method was selected because the Kriging model based optimization is very efficient for a design problem with multiple objectives and a small number of design variables.

A wide variety of techniques was applied to the present design optimization. Fig.1 shows the flowchart of the design process.

First, sample individuals (winglets) were selected from the design space. The method used to scatter points uniformly in the space is called ‘space-filling’. In this study, the Latin hypercube sampling (Ref.[11]) was used for the space-filling. This method ensures that a point always exists inside the interval partitioned by the number of sample points. A total of 32 sample individuals were selected from the initial search region. Fig.2 shows the initial sample individuals. A wide variety of winglet shape was considered in the design.

Unstructured Euler CFD analysis at Mach 0.80, 1G cruise CL was conducted for each winglet shape.

Navier-Sokes simulations are still expensive for three-dimensional design problems. Therefore, we chose Euler CFD for the design exploration and conducted a validation by Navier-Stokes analysis for the designed configurations. Euler CFD with the drag decomposition method has been successfully applied to the transonic drag evaluation in the past research (Ref.[12]-[14]). However, Euler CFD cannot capture the behavior of profile drag. Additional wetted area due to installation of the winglet will lead to additional profile drag. In this study, the profile drag was taken into accounted by a simple algebraic model and added to the inviscid drag. From CFD results, wave drag and induced drag were extracted using the mid-field drag decomposition technique. As for profile drag , the increase in the profile drag due to the additional wetted area of winglet was estimated with the following simple algebraic model

$$\Delta CD_p = k_w \cdot \Delta CD_f$$

$$\Delta CD_f = \left[\frac{0.455}{\left(\log_{10} \mathrm{Re}_c\right)^{2.58}} \left(1 + 0.15 M_\infty^2\right)^{-0.58} \right] \frac{\Delta S_{wet}}{S_{ref}}$$

$$k_w = 1 + \frac{2C_w (t/c) \cos^2 \Lambda_{w25}}{\sqrt{1 - M_\infty^2 \cos^2 \Lambda_{w25}}} + \frac{C_w{}^2 \cos^2 \Lambda_{w25} (t/c)^2 \left(1 + 5\cos^2 \Lambda_{w25}\right)}{2\left(1 - M_\infty^2 \cos^2 \Lambda_{w25}\right)}$$

where $C_w = 1.1$. ΔS_{wet} and Λ_{w25} are the additional wetted area and sweep angle at 25% chord of the winglet, respectively.

Also, the structural weight penalty of the wing box due to winglet installation was estimated by MSC NASTRAN™. Structural optimization of the wing box was performed to achieve minimum weight within the constraints of strength requirements. For the strength evaluation, the static load was calculated from the pressure distribution on the wing and winglet, which is computed by the Euler solver.

Then, block fuel and Max takeoff weight were evaluated by an in-house performance analysis tool. In this module, the wing box weight and aerodynamic drag were used as input. In the tool, drag was evaluated by the following formula:

$$CD = CD_p + CD_i + CD_w$$

$\Delta CD_p, \Delta CD_i, \Delta CD_w$ as derived from drag evaluation were added to the baseline (no winglet) drag and also the structural weight penalty ΔW was added to the baseline weight, then block fuel was estimated.

Max takeoff weight was estimated using the fuel carried derived from block fuel and structural weight.

Finally, design exploration and design decision were conducted using data mining techniques.

In the present study, we utilized the Kriging model, function analysis of variance (ANOVA) (Ref.[15]), and expected improvement (EI) (Ref.[16]).

In the entire design process shown in Fig.1, A brief introduction to each technology adopted in the present study is presented in the following sections

2.3 Geometry Definition

As the baseline geometry, wing-body configuration of a commercial jet aircraft was used. The winglet shape was defined by 6 variables as shown in Fig.3. Upper and lower limits of each design variable were defined by the statistical survey of existing aircrafts. Upper limit of the winglet cant angle is 84 deg, which means simple wing extension for the baseline wing with 6 degree-dihedral.

The airfoil section of the winglet was defined by that of the wing tip with the rule that t/c constant. At the wing-winglet junction, tangential smooth connection was achieved using a Bezier curve as shown in Fig.4

2.4 CFD solver and mesh

For the CFD solver, we used TAS (Tohoku University Aerodynamic Simulation) unstructured Euler code. Compressible Euler equations were solved with a finite-volume cell-vertex scheme. The numerical flux was computed using an approximate Riemann solver of Harten-Lax-van-Leer-Einfields-Wada (HLLEW) (Ref.[17]). Second-order spatial accuracy was achieved with a linear reconstruction of the primitive gas dynamic variables inside the control volume with Venkatakrishnan's limiter (Ref.[18]). The LU-SGS implicit method for unstructured meshes was used for the time integration (Ref.[19]).

The computational mesh for TAS code was generated automatically, and this reproducible mesh generation process greatly contributed to reducing numerical error in addition to drag decomposition method.

The number of nodes of using unstructured mesh was about 500 thousand in the current study.

The CFD computation in this study was executed by a master-slave type parallel computation using NEC SX-7 of Supercomputing System Information Synergy Center at Tohoku University. The 32 samples were evaluated by 32CPU in one execution and it took only 2hours.

2.5 Mid-Field drag decomposition method

To extract drag from calculated CFD results, the Mid-Field drag decomposition method (hereafter called near field method) was applied instead of wall boundary surface integration for accurate estimation and detailed investigation. By using the drag decomposition method, accurate drag prediction can be achieved by excluding the effect of unphysical entropy production. This has been validated coupled with TAS code for transonic flow in the previous work of the authors (Ref.[6]-[7]).

The mid-field method is derived from the far-field method by applying the divergence theorem. By using the divergence theorem, the entropy and enthalpy term of the far-field method can be transformed as follows:

$$CD_{(\Delta s,\Delta H)} = \iint_{WA} \vec{F}_{(\Delta s,\Delta H)} \cdot \vec{n} ds \cong \iiint_{V} \nabla \cdot \vec{F}_{(\Delta s,\Delta H)} dv$$

where WA is the trefftz plane and V is the flow field around the aircraft.

$\vec{F}_{(\Delta s,\Delta H)}$ is the entropy and enthalpy drag seed vector。

Drag decomposition of the entropy drag term is possible by domain decomposition of the flow field.

Then Eq.(3) can be transformed as follows:

$$CD_{(\Delta s,\Delta H)} = \iiint_{Vshock} \nabla\cdot\vec{F}_{(\Delta s,\Delta H)}dv + \iiint_{Vprofile} \nabla\cdot\vec{F}_{(\Delta s,\Delta H)}dv + \iiint_{Vspurious} \nabla\cdot\vec{F}_{(\Delta s,\Delta H)}dv$$
$$= CD_w + CD_p + CD_{sp}$$

The advantage of the mid-field method is that it can divide the entropy drag into the wave, profile and spurious drag components, and allow visualization of the generated positions and the strength of the drag in the flow field. The domain decomposition of flow field is based on the detective functions.

2.6 Structural weight estimation

Structural optimization of a wing box was performed to achieve minimum weight with constraints of strength requirements. Given the wing and winglet aero line for each individual, the finite element model of the wing box and winglet was generated automatically by in-house FEM generator for the structural optimization. Fig.5 shows a schematic view of the FEM model. The wing box model mainly consists of shell elements representing skin, spar and rib. Other wing components, such as control surfaces and subsystems are modeled using concentrated mass elements. Load transmission from winglet to the wing box was simulated with a rigid bar model. Winglet weight was considered as volume of a winglet multiplied by equivalent density of an existed winglet structure.

In the present structural optimization, strength is evaluated with using MSC NASTRAN^{TM}. Then, static analysis is conducted to obtain the stress on each element of the wing box. In the present study, as is well known, weight penalty is almost proportional to the wing-root bending moment as is shown in the following section. Therefore, such single point evaluation seemed enough for the derivation of the weight sensitivity to the wing-root bending moment change.

In the structural optimization, the thickness of shell elements is resized iteratively until the weight change converges sufficiently under the strength constraints.

2.7 Kriging model and Expected Improvement(EI)

The Kriging model is a method of Response Surface Model (RSM) which predicts unknown values from data observed at known locations. It minimizes the error of predicted values which are estimated by spatial distribution of the predicted values.

The Kriging model expresses the unknown function $y(\vec{x})$ as

$$y(\vec{x}) = \mu + Z(\vec{x})$$

where $\vec{x}$ is an m-dimensional vector (m design variables) , μ is a constant global model and $Z(\vec{x})$ represents a local deviation at an unknown point $\vec{x}$ expressed using stochastic process. The sample points are interpolated using the Gaussian random function as the correlation function to estimate the trend of the stochastic processes.

Then in order to find the global optimum in the Kriging model, both the estimated function value and the uncertainty at the unknown point are considered at the same time. Based on these values, the point having the largest probability of being the global optimum is found. The probability of being the global optimum is expressed by the criterion 'expected improvement (EI)'. The EI in a minimization problem is expressed as follows:

$$E(I) = s\int_{-\infty}^{f_{\min}^n} (f_{\min} - z)\phi(z)dz$$

where $f_{\min}^n = \frac{y_{\min} - \hat{y}}{s}$, $z = \frac{y - \hat{y}}{s}$ and

$$I(\vec{x}) = \begin{cases} [y_{\min} - y(\vec{x})] & \text{if } y(\vec{x}) < y_{\min} \\ 0 & otherwise \end{cases}$$

2.8 Function analysis of variance

In order to identify the effect of each design variable on the objective functions, the total variance of the model is decomposed into the variance component due to each design variable. This is called the functional analysis of variance (ANOVA). The decomposition is accomplished by integrating variables out of the model $\hat{y}$. The total mean $(\hat{\mu}_{total})$ and variance $(\hat{\sigma}_{total}^{\ 2})$ of model $\hat{y}$ are as follows:

$$\hat{\mu}_{total} = \int\cdots\int \hat{y}(x_1,.....,x_n)dx_1\cdots dx_n$$

$$\hat{\sigma}^2_{total} = \int \cdots \int [\hat{y}(x_1,.....,x_n) - \hat{\mu}]^2 dx_1 \cdots dx_n$$

The main effect of variable x_i is

$$\mu_i(x_i) = \int \cdots \int \hat{y}(x_1,.....,x_n) dx_1 \cdot\cdot dx_{i-1} dx_{i+1} \cdot\cdot dx_n - \hat{\mu}$$

The two-way interaction of variance x_i and x_j is

$$\mu_{i,j}(x_i, x_j) = \int \cdots \int \hat{y}(x_1,.....,x_n) dx_1 \cdot\cdot dx_{i-1} dx_{i+1} \cdot\cdot dx_{j-1} dx_{j+1} \cdot\cdot dx_n - \hat{\mu}_i(x_i) - \hat{\mu}_j(x_j) - \hat{\mu}$$

The variance due to the design variable x_i is

$$\int [\mu_i(x_i)]^2 dx_i$$

The proportion of the variance due to design variable x_i to total variance of model can be expressed by dividing Eq.(26) by Eq.(24)

$$\frac{\int [\mu_i(x_i)]^2}{\int \cdots \int [\hat{y}(x_1,.....,x_n) - \hat{\mu}]^2 dx_1 \cdots dx_n}$$

This value indicates the sensitivity of the model to the variation of each design variable

3 Multi-Disciplinary Design Exploration

3.1 Aerodynamic effects of winglet

From the CFD analysis of 32 sample individuals, detailed aerodynamic effects of winglet were extracted. Incremental value for the baseline wing-body (no winglet) was evaluated, so herein after Δ denotes the increment from the baseline.

As shown in Fig.6, wing-root bending moment increase is linearly related to drag reduction, which shows the trade-off between aerodynamic performance and weight penalty.

To obtain detailed understanding of the aerodynamic effects of each variable, the Kriging model was utilized for a function approximation. and the ANOVA is performed. Design variables and their interactions (covariance) including their proportion to the total variance is shown from Fig.7. From this figure, we can draw the following conclusions regarding the winglet design.

· For drag reduction, winglet span length and cant angle are the dominant parameters

· Winglet span is dominant in induced drag, while cant angle is dominant in wave drag.

· For wave drag reduction, covariance is significant which requires good tailoring of all parameters.

· For wing-root bending moment, winglet span and cant angle are still dominant, however, the sensitivity of other parameters are larger compared with drag.

3.2 Weight and Aircraft performance analysis

Structural optimization for 32 points was conducted and structural wing box weight was estimated. Fig.8 shows the relationship between wing box weight and wing root bending moment. As was expected, structural weight has a strong linear dependence on wing root bending moment in this design problem.

Then, aircraft performance was estimated from obtained drag and weight data. Fig.9 shows estimated performance chart. The figure contains wing box weight, drag, block fuel and MTOW. In the figure, wing box weight was divided by the MTOW of baseline. Block fuel reduction due to winglet in the current design space is from 2% to 5%. Structural weight penalty is from 0.5% to 3.5%, while MTOW increase is within 2%, which is because fuel carried decreases due to block fuel improvement.

As the next step, Kriging model was constructed for block fuel and MTOW as a function of 32 sample points, then, Pareto front was derived through the minimization of both objectives in the Kriging model by Multi-Objective Genetic Algorithm (MOGA, Ref.[8]).

Fig.10 shows estimated Pareto front. As seen in the figure, there is a trade-off between block fuel improvement and MTOW reduction.

3.3 Design decision

From the detail investigations so far, the final candidate for the winglet shape was decided. Past researchers had derived the Pareto front or sensitivity information for MDO problems. However, the design decision is not so straightforward that a single candidate can be clearly chosen from the obtained Pareto front. Many factors affect the decision in the practical

design situation. It is very natural that all factors that affect the decision cannot always be covered with numerical optimizations. In the present study, low speed aerodynamic characteristics, flutter characteristics and the aesthetic standpoint were not covered. So, design decisions should be made coupled with MDO results with such uncovered information. Present design processes based on Kriging approximation is very capable for such a point of view compared with other optimization algorithms such as gradient base optimization. The present process is developed to reveal the whole structure of the design space utilizing various sensitivities and trade-off information, not to give optimal solutions. Therefore, it is so flexible as to handle with the uncovered information.

In the present study, EI is utilized for the decision. EI maximization on the Kriging model was conducted by MOGA. Fig.11 shows examples of normalized EI distributions for block fuel and MTOW as a function of design variables. Where, An EI value of 1 means most probable for minimization of objective function. In the figure, for the sweep angle, there are some optimum values for both objective functions around 35deg. For the winglet span length, there is a clear trade-off between two objective functions. For the winglet taper ratio, both objective functions don't have clear dependency.

The decision was made from the EI and some additional criteria for uncovered design consideration.

Of course, the criteria depend on the strategy of the designers. Examples of the decision criteria for the present study are as follows:

(a)Smaller cant is lower risk for low speed stall and buffet characteristics.

(b)Larger toe out angle is lower risk for flutter characteristics.

(c)Smaller taper ratio and moderate cant angle are better from the aesthetic standpoint.

(d)Landing fee dependence on MTOW should be equal category to the baseline.

(e)The difference from the Pareto front should be minimized.

We determined each design variable so as to maximize EI as much as possible, considering trade-off between the Pareto front and the criteria above. As a result, one candidate was selected (herein after 'designed' winglet). Also, one winglet, which has smaller cant and larger chord length than those of the designed winglet as the representative of the conventional winglet, was selected for comparative use (herein after 'conventional' winglet). Fig.12 shows the designed winglet configuration and Fig.13 shows the conventional one.

Fig.14 shows the comparison of block fuel and MTOW among designed, conventional and Pareto front. From the figure, designed winglet configurations have almost equivalent performance with Pareto front, while, the conventional one has no MTOW penalty and 1% block fuel deterioration from the Pareto front

4 Validation

4.1 Validation of the Kriging approximation

In the present study, validity of the design depends on the accuracy of drag estimation, weight estimation and Kriging model approximation. As for the Kriging model, one of the advantages is its ability to control the accuracy of the approximation. If necessary, the accuracy of the approximation is easily augmented by using additional samples by some criteria, such as EI maximization of an objective function.

To validate the approximation, comparison of aerodynamic characteristics between approximations and Euler CFD results for two selected winglets was conducted. Table 1 shows the result of this comparison. The result was sufficient. The difference was 1 drag counts and 0.1% for wing root bending moment.

Therefore, we found that 32 sample points were enough for the present study

4.2 Validation of the aerodynamics design by Wind Tunnel Test

To validate the aerodynamic design of the winglet, a wind tunnel test was conducted as a part of a preliminary development wind tunnel

test. The wind tunnel used was JAXA 2m×2m continuous transonic wind tunnel (Ref.[20]) in Japan. The model we used was a 3.4% scale model and had Reynolds number based on MAC of about 1.2million at design Mach number. Six-component aerodynamic forces and moments were measured by an internal balance.

In the winglet design phase aerodynamic drag was evaluated by Euler CFD analysis from efficient design standpoint. Of course Euler CFD neglects viscous effects and may lead to misunderstanding of the actual design sensitivities. Therefore, Navier-Stokes (NS) analysis were also conducted in addition to Euler analysis for comparative use. For NS analysis, unstructured hybrid mesh (Ref.[21]) and Spalart-Allmaras turbulence model (Ref.[22]) was applied. Meshes used for NS analysis were approximately 1.3 million nodes for the baseline and 1.9 million nodes for the winglet configuration. For the drag evaluation of NS analysis, mid-field drag decomposition method, the same as for Euler analysis was applied.

Fig.15 shows the comparisons of drag reduction due to the winglet installation as an increment from the baseline (without winglet). Present design was validated through the well agreement among Euler, NS and WTT results.

The designed winglet was also tested in a low speed wind tunnel to determine the low speed aerodynamic characteristics. In the low speed test, improvement of lift to drag ratio at takeoff configuration and no degradation of maximum lift and pitch characteristics was validated

5 Conclusion

In this paper, we report on a multi-disciplinary design exploration for winglet was conducted for advanced winglet design in the practical aircraft design.

Minimization of block fuel and Max takeoff weight were selected as design objectives. Both objectives were derived from CFD based aerodynamic drag and FEM based structural weight utilizing various CFD and optimization techniques.

As for CFD analysis, Mid-field drag decomposition method and automatic mesh generation, which contributes to keeping mesh quality constant, were applied for accurate drag evaluation. Also, thanks to the parallel CFD computations, the design completed within a day.

Aerodynamic and structural design information of winglet configuration was obtained from the design exploration in the design space based on 32 individuals of winglet configuration utilizing Kriging function approximation and its analysis of variance. In addition to the well known effectiveness, such as the effectiveness of winglet span length to induced drag and to bending moment, other important effectiveness such as that of winglet cant angle to wave drag reduction was obtained.

Large cant angle of the winglet was found to be favorable for both block fuel and Max takeoff weight in the present study from the obtained the Pareto front.

Then, the practical design decision was explored by coupling the obtained design information with some design criteria, which were uncovered within the present numerical optimization. The decision based on EI maximization was found to be very useful for the practical complex design problem.

Finally, Kriging function approximation, which was the foundation of the present design decision, was validated. Also, aerodynamic drag was validated by the wind tunnel results. Therefore, present design was validated.

Acknowledgements

This research was conducted under the financial support of NEDO (New Energy and Industrial Technology Development Organization). The authors would like to express special thanks to Professor Obayashi, Dr Jeong of Institute of Fluid Science, Tohoku university and Mr. Morino of MHI for their sincere cooperation in the present work. Also, we would like to express special thanks to Dr. Ito of the University of Alabama at Birmingham for his cooperation in the automatic mesh generation tool development

References

[1] Whitcomb, Richard T., A Design Approach and Selected Wind-Tunnel Results at High Subsonic

Speeds for Wing-Tip Mounted Winglets," NASA TN D-8260, June 1976.

[2] Smith, Stephen C., "Trefftz-Plane Drag Minimization at Transonic Speeds," SAE Paper 971478, April 1997.

[3] Iran, K.," Nonplanar Wing Concepts for Increased Aircraft Efficiency," VKI lecture series on Innovative Configurations and Advanced Concepts for Future Civil Aircraft, June, 2005.

[4] Kusunose, K., "A Wake Integration Method for Airplane Drag Prediction," The 21st Century COE Program International COE of Flow Dynamics Lecture Series, Vol.3, 2005.

[5] Schmitt, V., and Destarac, D., "Recent Progress in Drag Prediction and Reduction for Civil Transport Aircraft at ONERA," AIAA Paper 98-0137, 1998.

[6] Yamazaki, W., Matsushima, K., and Nakahashi, K., "Application of Drag Decomposition Method to CFD Computational Results," AIAA Paper 2005-4723, 2005.

[7] Yamazaki, W., Matsushima, K., and Nakahashi, K., "Unstructured Mesh Drag Prediction Based on Drag Decomposition," ECCOMAS CFD 2006, 2006.

[8] Oyama, A., Obayashi, S., Nakahashi, K., and Hirose, N.,"Aerodynamic Wing Optimization via Evolutionary Algorithms Based on Structured Coding," Computational Fluid Dynamics Journal, Vol. 8, No. 4, 2000, pp. 570–577.

[9] Kim, H.J., and Nakahashi, K., "Aerodynamic Design Optimization Using Unstructured Navier-Stokes Equations and Adjoint Method," ICAS2004-2.7.5, Yokohama Japan, Aug. 29 - Sept.3 2004.

[10] Jeong, S., J., Murayama, M. and Yamamoto K., "Efficient Optimization Design Method Using Kriging Model," AIAA paper 2004-0118.

[11] Mckay, M. D., Beckman, R. J. and Conover, W. J., "A Comparison of Three Methods for Selecting Values of Input Variables in the Analysis of Output from a Computer Code," Technometric, Vol. 21, No. 2, 1979, pp. 239-245.

[12] van Dam, C. P., Nikfetrat, K.,Wong, K., and Vijgen, P. M. H.W., "Drag Prediction at Subsonic and Transonic Speeds Using Euler Methods," Journal of Aircraft, Vol. 32, No. 4, 1995, pp. 839–845.

[13] van Dam, C. P., and Nikfetrat, K., "Accurate Prediction of Drag Using Euler Methods," Journal of Aircraft, Vol. 29, No. 3, 1992, pp. 516–519.

[14] van Dam, C. P., "Recent Experience with Different Methods of Drag Prediction," Progress in Aerospace Sciences, Vol. 35, No. 8, 1999,pp. 751–798.

[15] Donald, R. J., Matthias S and William J. W, "Efficient Global Optimization of Expensive Black-Box Function," Journal of global optimization, Vol. 13, 1998, pp. 455-492.

[16] Matthias, S., William, J. W. and Donald, R. J., "Global Versus Local Search in Constrained Optimization of Computer Models," New Developments and Applications in Experimental Design, edited by N. Flournoy, W.F. Rosenberger, and W.K. Wong , Institute of Mathematical Statistics, Hayward, California, Vol. 34, 1998, pp. 11-25.

[17] Obayashi, S. and Guruswamy, G. P., "Convergence Acceleration of an Aeroelastic Navier-Stokes Solver," AIAA Journal, Vol. 33, No. 6, 1994, pp. 1134–1141.

[18] Venkatakrishnan, V., "On the Accuracy of Limiters and Convergence to Steady State Solutions," AIAA Paper 93-0880, 1993.

[19] Sharov, D. and Nakahashi, K., "Reordering of Hybrid Unstructured Grids for Lower-Upper Symmetric Gauss-Seidel Computations," AIAA Journal, Vol. 36, No. 3, 1998, pp. 484–486.

[20] JAXA website, "URL: http://www.iat.jaxa.jp/res/wintec/0b00.html"

[21] Ito, Y. and Nakahashi, K., "Improvements in the Reliability and Quality of Unstructured Hybrid Mesh Generation, "International Journal for Numerical Methods in Fluids, Vol. 45, Issue 1, 2004, pp. 79–108.

[22] Spalart, P. R. and Allmaras, S. R., "A One-Equation Turbulence Model for Aerodynamic Flows", AIAA-92-0439, Jan.1992

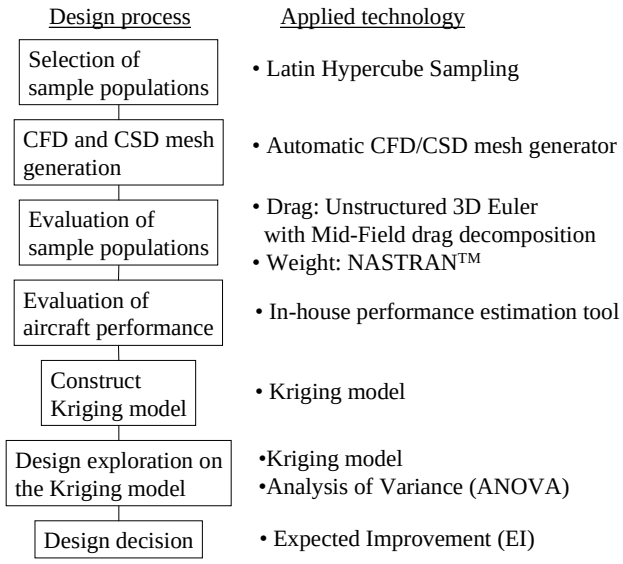

Fig.1 Design flow chart

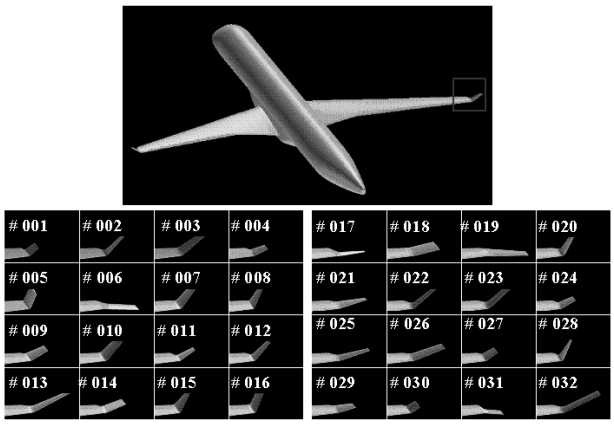

Fig.2 Winglet shape of sample individuals

(backward view)

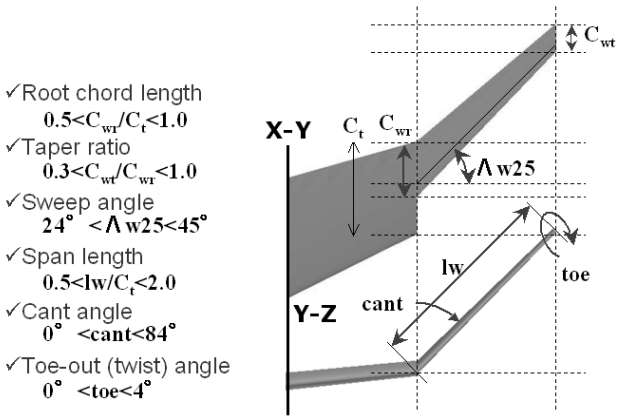

Fig.3 Winglet shape definition

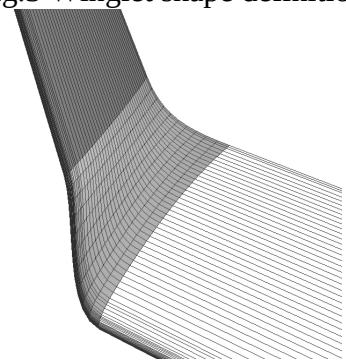

Fig.4 Enlarged view of wing-winglet junction

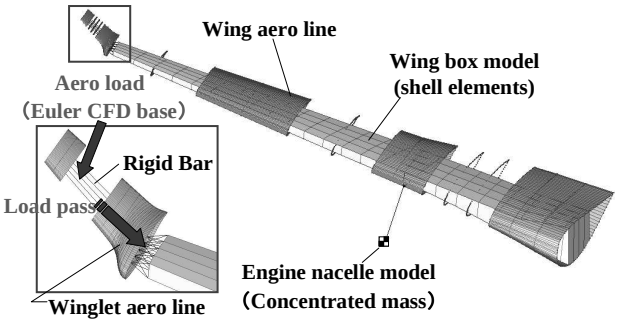

Fig.5 Schematic view of FEM model for wing with winglet configuration

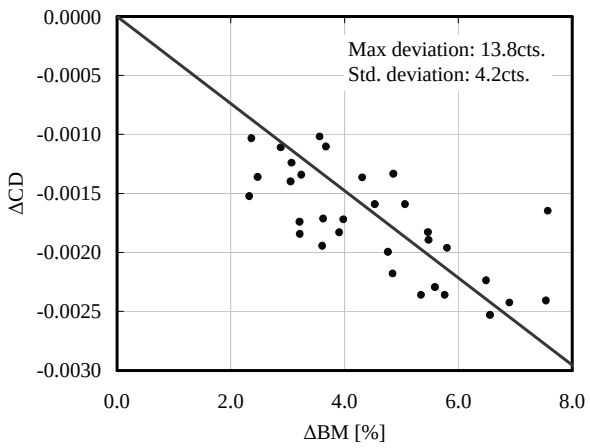

Fig.6 Relationship between drag and wing-root bending moment

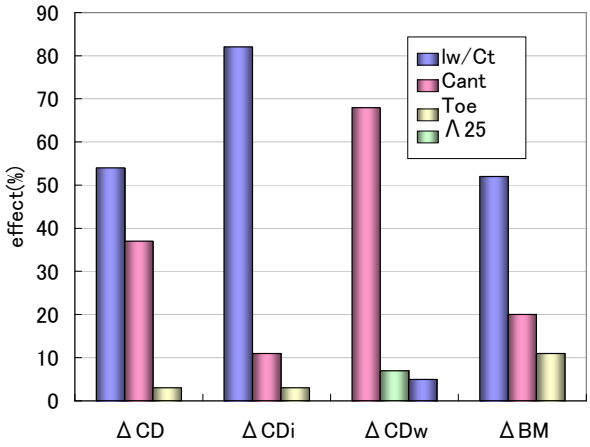

Fig.7 ANOVA results for each drag component

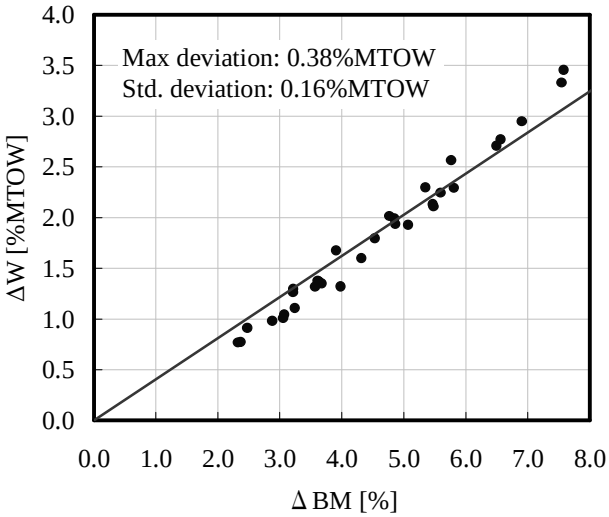

Fig.8 Relationship between wing box weight and wing root bending moment

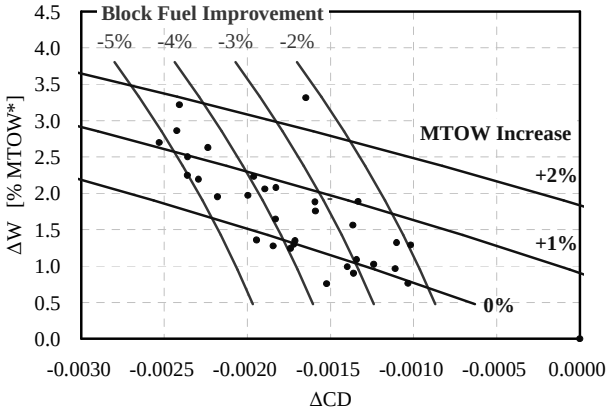

Fig.9 Estimated aircraft performance chart

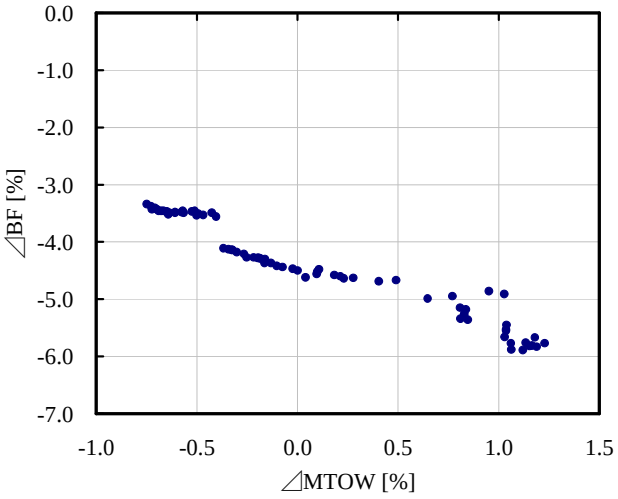

Fig.10 Estimated Pareto front

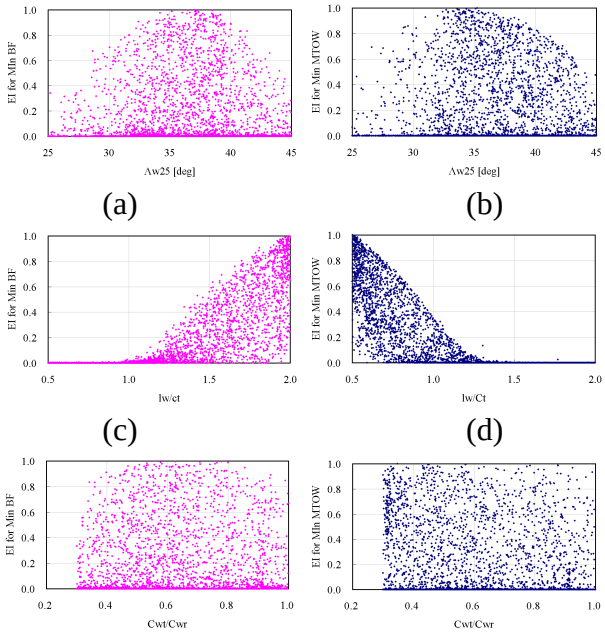

Fig.11 Normalized EI for block fuel and MTOW as a function of design variables

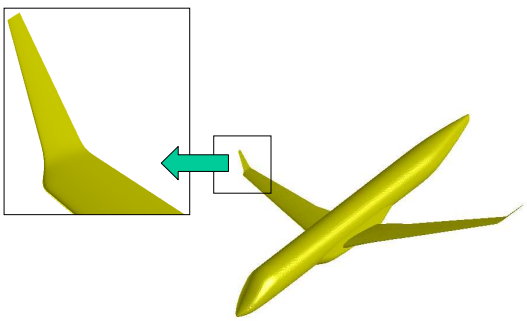

Fig.12 Designed winglet configuration

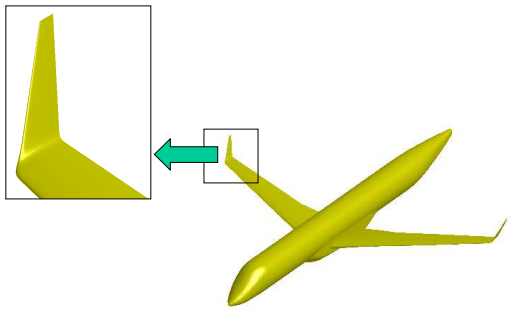

Fig.13 Conventional winglet configuration

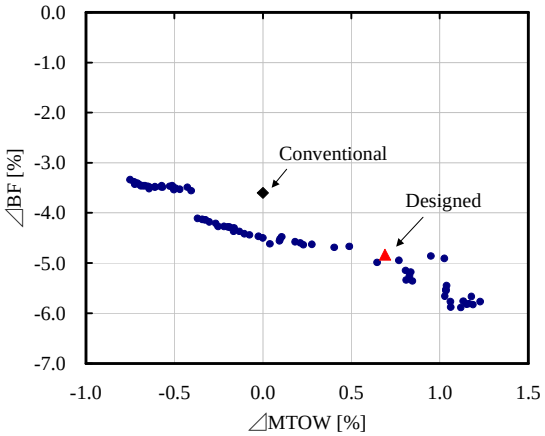

Fig.14 Comparison among selected configurations and Pareto front

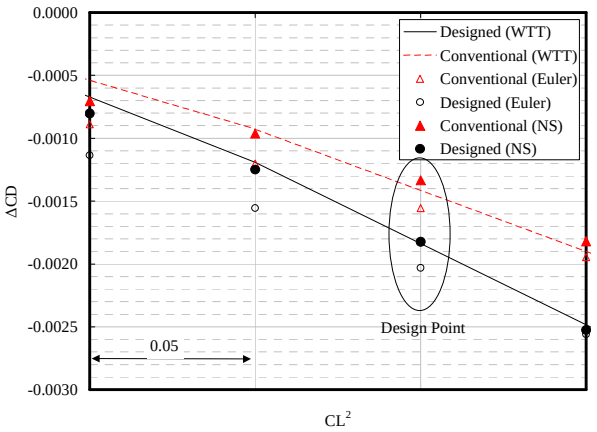

Fig.15 Comparisons of drag reduction due to the winglets

Copyright Statement